



ELSEVIER

Journal of Alloys and Compounds 319 (2001) 108–118

Journal of
ALLOYS
AND COMPOUNDS

www.elsevier.com/locate/jallcom

Field activated combustion synthesis of the silicides of vanadium

F. Maglia^a, U. Anselmi-Tamburini^{a,*}, C. Milanese^a, N. Bertolino^b, Z.A. Munir^b^aDepartment of Physical Chemistry and C.S.T.E./CNR, University of Pavia, V.le Taramelli, 16, 27100 Pavia, Italy^bDepartment of Chemical Engineering and Materials Science, University of California, Davis, CA 95616-5294, USA

Received 1 November 2000; accepted 18 November 2000

Abstract

The synthesis of vanadium silicides was investigated using the field-activated combustion synthesis technique. For all V–Si compounds, self-sustaining combustion reactions could be obtained when fields above a threshold value were imposed. Monophasic products were obtained only for the starting compositions V:Si=1:2 and V:Si=5:3. For all other compositions the reaction produced a polyphasic mixture. No significant variation of phase composition was observed with an increase in field strength. In contrast with other systems, the field was seen to have a weak effect on the combustion macrokinetic parameters. This was interpreted on the basis of the large electrical conductivity of the reaction products, driving a large part of the electric flux away from the reaction front. The reaction mechanism was investigated through the use of quenching experiments. Only the VSi_2 and V_5Si_3 phases were observed in the leading edge of the combustion front, with the other phases forming from solid–solid interactions in the afterburn. These results have been compared with observations relative to the mechanism of silicides formation in isothermal solid–solid and solid–liquid diffusion couples. © 2001 Elsevier Science B.V. All rights reserved.

Keywords: Ceramics; Chemical synthesis; X-ray diffraction; Diffusion; Silicides, intermetallics

1. Introduction

The high-temperature oxidation resistance and attractive mechanical properties of the transition metal silicides have generated considerable interest in their potential use in high-temperature applications and in aggressive environments. Their relatively low electric resistivity and good compatibility with silicon substrates have made them attractive for use as contacts or interconnects in electronic applications. A number of alternative routes have been employed over the past 30 years for the bulk synthesis of transition metals silicides. Among these, the method of combustion synthesis has been shown to be suitable for the synthesis of those silicides with a large negative enthalpy of formation, e.g. MoSi_2 , Ti_5Si_3 , and Zr_5Si_3 [1–8]. Many other silicides, however, cannot be obtained through this method due to their relatively low heat of formation. Recently a modification of the classical approach, called field activated combustion synthesis (FACS), has been

shown to be effective in the synthesis of several low-exothermic silicides such as NbSi_2 , TaSi_2 , WSi_2 , CrSi_2 and Cr_5Si_3 [9–14]. The FACS method is based on the application of an electric field perpendicular to the direction of propagation of the combustion wave. The resulting current flowing through the reacting mixture provides Joule heating at a rate of σE^2 with σ being the conductivity and E the field. Depending on the electrical conductivity of reactants and products, the added electrical energy can be confined to the reaction zone, thus providing maximum activation to the self-sustaining reaction process.

In this paper we report on the synthesis of vanadium silicides by the FACS method. No previous results on the combustion synthesis of vanadium silicides have been reported. In fact, the low enthalpies of formation of the V–Si compounds coupled with their relatively low melting points make their synthesis by the normal SHS method difficult or impossible. The microscopic reaction mechanism involved in the field-assisted combustion process is investigated through the analysis of quenched experiments. Because no previous information was available on the kinetics of the reactions in the V–Si system, solid-state diffusion couples and solid–liquid interaction experiments

*Corresponding author. Tel.: +39-0382-507-208; fax: +39-0382-507-575.

E-mail address: tau@chifs.unipv.it (U. Anselmi-Tamburini).

were also performed. The aim of this study was to provide a better understanding of the role of the various elementary processes involved in the microscopic mechanism of the combustion reaction.

2. Experimental

2.1. Field-activated combustion synthesis experiments

Powder mixtures were prepared from elemental V (Alfa, –325 mesh, 99.5% pure) and Si (Alfa, –325 mesh, 99.5% pure) by manual dry mixing. Green pellets were produced by cold isostatic pressing of the powder mixtures into rhombohedrally shaped samples with a length of 21 mm, a width of 6.8 mm, and a height varying between 10 and 11 mm. The pellets were placed inside a stainless steel reactor between two spring-loaded graphite electrodes, across which a voltage was applied. The electrodes were in contact with the long faces of the pellets. Ignition was achieved through an electrically heated tungsten coil placed at 1–2 mm from one end of the sample. This experimental geometry provides an electric field perpendicular to the expected direction of wave propagation. All the experiments were performed in a high purity argon (99.998%) atmosphere. Temperature profiles were measured with a two-color pyrometer (Ircon Modline R-99C15) focused on the middle portion of the sample. Combustion wave velocities were determined by a video recorder equipped with a time-code generator. The instantaneous current and voltage passing through the sample were measured in real time during wave propagation. More details on the experimental apparatus are given elsewhere [9–12].

Structural and microstructural characterization of the combusted samples was obtained through scanning electron microscopy (SEM) and powder X-ray diffraction analyses (XRPD). For the SEM analyses a Cambridge Stereoscan 200 SEM (operated at 30 kV and equipped with a back-scattered detector and a Link microprobe) was used. The surface of the samples was coated with either 20 nm of sputtered gold or evaporated graphite. XRPD analyses were performed using a Phillips 1710 diffractometer equipped with a copper anode operated at 40 kV and 35 mA, graphite curved monochromator on the diffracted beam, and a proportional counter.

2.2. Diffusion couple experiments

Bulk diffusion couples were prepared using slices of V and Si, 5 mm in diameter \times 1–2 mm thick. Prior to assembling, the mating surfaces of the V and Si slices were prepared by grinding with 1200 and 2400 grit silicon carbide metallographic papers, polishing with 1 μ m diamond paste, and cleaning with acetone. The cleaned V and Si slices were then pressed tightly together between

spring loaded alumina rods inside an alumina tube and placed in a furnace under a high purity argon flux.

The diffusion couples were annealed at temperatures of 1150, 1250 and 1350°C for times ranging from 4 to 32 h. After cooling, the samples were mounted in epoxy, sectioned, polished, and examined by optical and electron microscopy. The composition of the reacted zone was determined by electron microprobe analysis (EMPA).

2.3. Solid–liquid interaction experiments

Interactions between solid V and liquid Si were performed at 1460°C for relatively short times (up to 10 min). The experiments were carried out inside an alumina crucible. A piece of V was covered with loose Si powder and then placed in a high temperature furnace under a high purity argon flux. At the end of the interaction time the system was quenched by pushing the crucible outside the hot zone of the furnace.

3. Results

3.1. Field-activated combustion synthesis

The phase diagram of the V–Si system, Fig. 1, shows the presence of four intermetallic compounds, VSi_2 , V_6Si_5 , V_5Si_3 and V_3Si . With the exception of V_6Si_5 , all the compounds show a congruent melting point. No significant solubility of vanadium in solid silicon can be observed but a limited (up to 6.5 at.%) solubility of Si in solid vanadium is reported. Four eutectics are present in this binary. The eutectic richest in Si is very close in both composition (3 at.% Si) and in temperature (1400°C) to pure Si (m.p. = 1414°C). Some features of this phase diagram, however, are still not well established. The limit of existence of the V_6Si_5 phase, for instance, is known only with a large uncertainty (1160 \pm 100–1670°C).

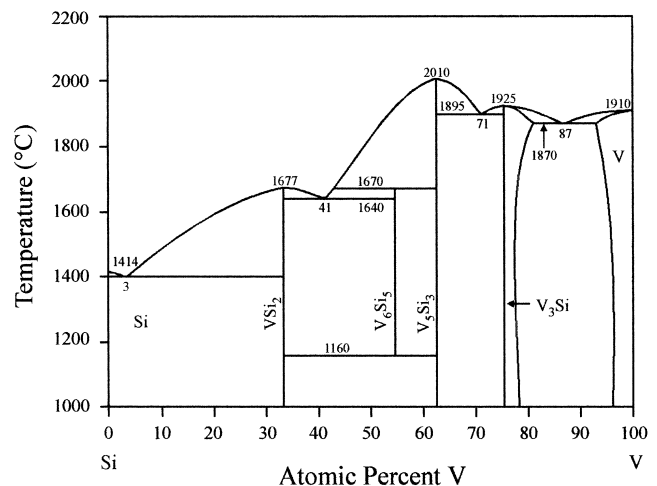


Fig. 1. Phase diagram for the V–Si system.

Table 1

Enthalpies of formation, crystal structures, and adiabatic combustion temperatures for the silicides of vanadium

| Compounds | Crystal structure | ΔH_{f298} (kJ/mol of atoms) [15] | T_{ad} (K), $T_0 = 298$ |
|---|---------------------------|--|---------------------------|
| VSi ₂ | <i>P6₃22</i> | -40.7 | 1827 |
| V ₆ Si ₅ | <i>Immm</i> | -49.6 | - |
| V ₅ Si ₃ | <i>I4/mcm</i> | -53.8 | 1792 |
| V ₅ Si ₃ ^a | <i>P6₃/mcm</i> | -53.8 | 1792 |
| V ₃ Si | <i>Pm3n</i> | -43.1 | 1664 |

^a Hexagonal metastable form. Stabilized by the presence of small amount of C, O, and N.

Published ΔH_{298}^0 of formation values for the vanadium silicides are listed in Table 1 [15]. Table 1 also shows the adiabatic combustion temperatures (T_{ad}) calculated for all the phases with known enthalpies and heat capacity, C_p , values. The T_{ad} values, which range from 1664 to 1827 K, lie below or near the empirical limit of 1800 K which is generally recognized as a good indicator of the occurrence of self-propagating processes.

FACS experiments were performed using powder mixtures with starting compositions corresponding to all the intermetallic compounds present in the V–Si phase diagram: V:Si = 1:2, V:Si = 6:5, V:Si = 5:3 and V:Si = 3:1. In the absence of a field, only the composition V:Si = 5:3 reacted in a self-propagating mode. On the other hand, when an appropriate field is applied, all the compositions produced stable combustion fronts. However, combustion waves were propagated only when the field was above a threshold value which depended on composition: 10, 14 and 9 V cm⁻¹ for the compositions V:Si = 1:2, V:Si = 6:5 and V:Si = 3:1, respectively. Once ignited, the V:Si = 1:2 and V:Si = 6:5 mixtures reacted completely at any field above the threshold, while for the V:Si = 3:1 the front never reach the end of the pellet even at the highest applied field, but the reacted fraction linearly increased with field strength from 55% at 14 V cm⁻¹ to 72% at 22 V cm⁻¹.

With the exception of the composition V:Si = 1:2 no significant dependence of the reaction wave temperature and propagation rate on the strength of the applied field was observed. For the 1:2 stoichiometry the reaction temperature increased from 1390 to 1561°C as the field was increased from 10 to 18.5 V cm⁻¹, as can be seen in Fig. 2. For the composition V:Si = 5:3 the reaction temperature was around 1600°C for all voltages applied, while that for the V:Si = 6:5 and V:Si = 3:1 compositions was around 1480°C.

Reaction front velocities generally show a slight increase with an increase in the applied field intensity for all the starting mixtures, as seen in Fig. 3. Also in this case, the composition V:Si = 1:2 shows a more pronounced variation.

Despite the weak effect on the maximum reaction temperature, the intensity of the applied field plays an important role in defining the overall temperature history

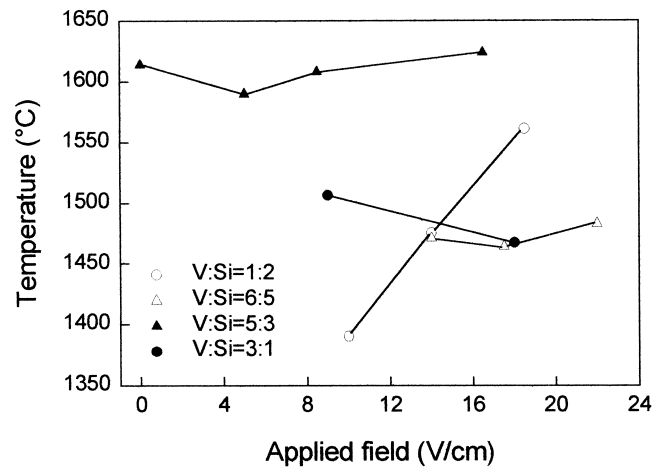


Fig. 2. Dependence of the maximum reaction temperature on the applied field strength.

of the samples. In fact, Joule heating due to the passage of the current flux tends to reduce the cooling rate as exemplified by Fig. 4 in which two temperature profiles, corresponding to two different values of the applied field for the composition V:Si = 3:1 are shown. This consideration plays a significant role in defining the phase composition of the final products, as the residence time of the sample at high temperature is considerably increased when the intensity of the applied field is increased.

Fig. 5 shows an example of the changes in the applied voltage and current during a typical FACS experiment. This example is for the combustion of a V:Si = 5:3 mixture at an applied field of 8.5 V cm⁻¹. Prior to ignition no measurable current flows through the compact due to the very low electrical conductivity of the mixture. As the combustion process starts (with time corresponding to point A) the current increases abruptly and the voltage decreases correspondingly. The current continues to increase until the combustion front reaches the end of the

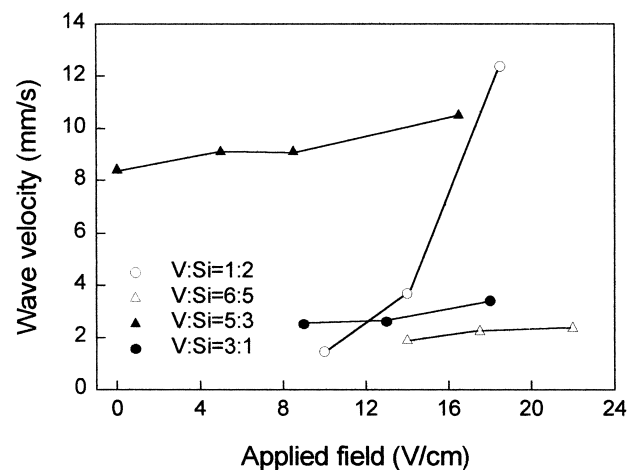


Fig. 3. Dependence of the combustion wave velocity on the applied field strength.

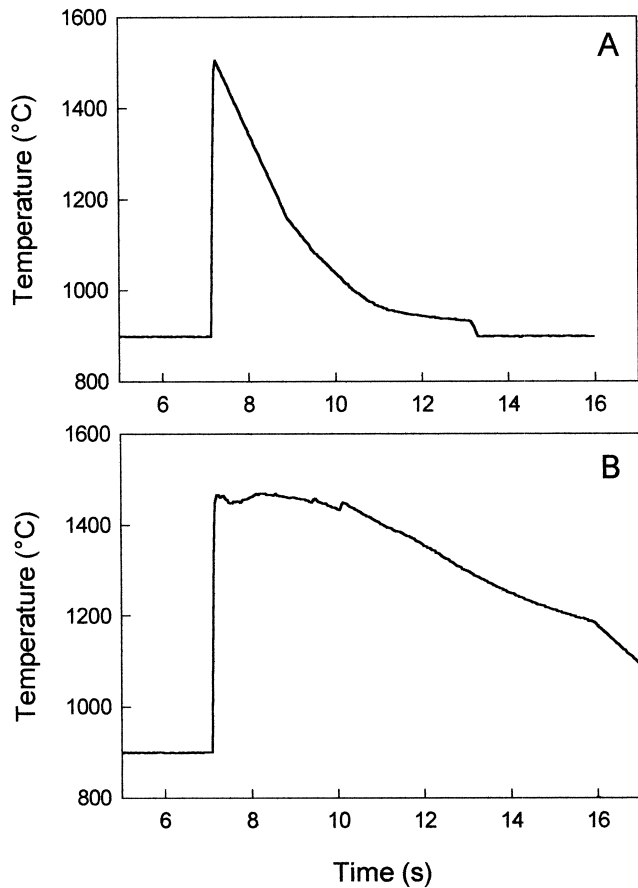


Fig. 4. Temperature profiles corresponding to the composition V:Si=3:1 reacted at two different field strengths (A) 13 V/cm, (B) 18 V/cm.

sample (point B in the figure). Voltage–current profiles for the reactions involving the V:Si=6:5 and in particular the V:Si=1:2 mixtures were generally much more irregular because the products partially melted, causing sample deformation and irregularity in the contacts with the electrodes.

The phase composition of the reaction final products

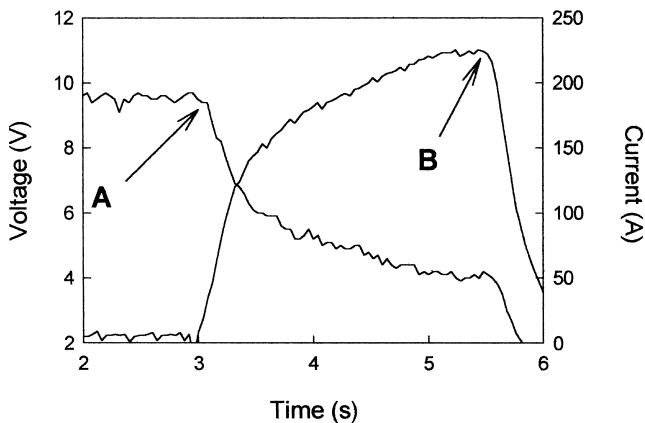


Fig. 5. Time dependence of the current and voltage during wave propagation in the synthesis of V_5Si_3 . (A) Ignition (B) extinction.

was determined by XRPD. The results are summarized in Figs. 6–9 for the starting compositions (V:Si) of 1:2, 5:3, 6:5 and 3:1, respectively. In these figures the patterns labeled 1, 2 and 3 represent results obtained with different applied fields as indicated in the respective captions. In several cases the product was nearly a pure single phase. The composition V:Si=1:2, for example, resulted in the formation of VSi_2 , with only traces of V_5Si_3 and Si for any value of the applied field above the threshold (Fig. 6). Similarly, the composition V:Si=5:3 gave an almost single phase product. In this case the tetragonal modification of the V_5Si_3 (hereafter $t-V_5Si_3$) phase was obtained as the major component with only traces of the metastable hexagonal form (hereafter $e-V_5Si_3$). Also in this case, the phase composition was independent of the applied field strength (Fig. 7). It should be recalled that this composition is the only one producing self-propagating reactions in the absence of an electric field. No appreciable difference in product phase composition was observed, regardless of the presence or absence of the field. In contrast to these two compositions, the V:Si=6:5 composition generated a large number of phases which occurred in comparable amounts. The product contained the phases $t-V_5Si_3$, $e-V_5Si_3$, V_6Si_5 , V_3Si , and VSi_2 . Although there were small differences in the relative amounts of the phases for different field values, a clear trend is not discernible, as can be seen in Fig. 8. In contrast, a clear variation in the product composition with the field strength was observed for the starting composition V:Si=3:1. The phase V_3Si was always the major component, but at low fields the product contains a significant amount of $t-V_5Si_3$ which diminishes as the field is increased, Fig. 9.

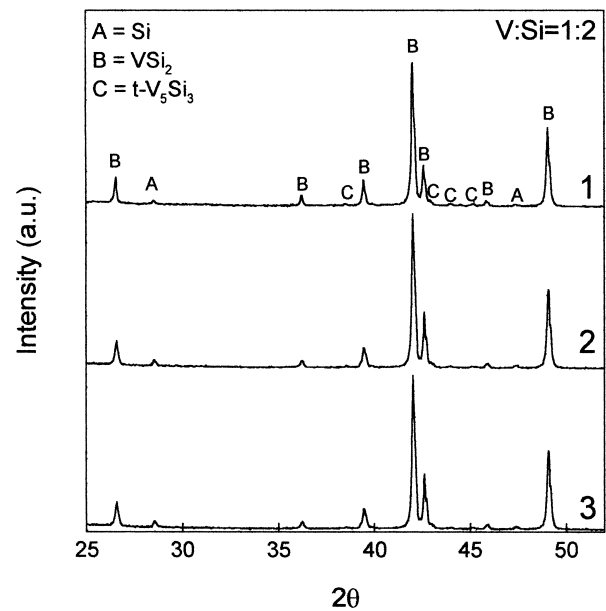


Fig. 6. X-ray powder patterns for the FACS reaction products corresponding to the composition V:Si=1:2. (1) 10 V/cm, (2) 14 V/cm and (3) 18.5 V/cm.

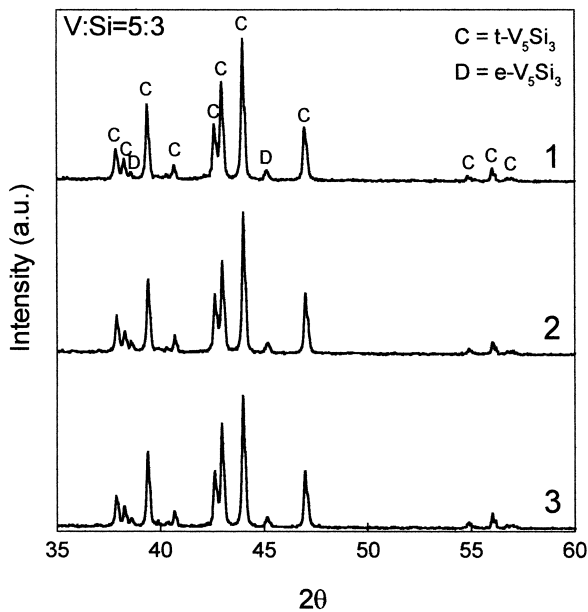


Fig. 7. X-ray powder patterns for the FACS reaction products corresponding to the composition V:Si=5:3. (1) 0 V/cm, (2) 8.5 V/cm and (3) 16.5 V/cm.

3.2. Quenching experiments

In some experiments the voltage was abruptly reduced to zero after the wave had propagated halfway through the sample. The wave was rapidly extinguished as a result of this action. In these experiments, coarser vanadium powders were used in part to facilitate SEM/EMPA analyses of the product phases evolution (producing larger microstructures), and in part to allow for the quenching of all

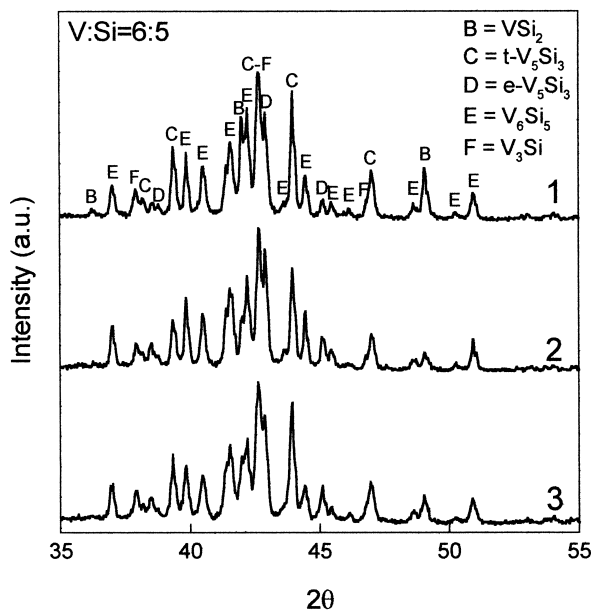


Fig. 8. X-ray powder patterns for the FACS reaction products corresponding to the composition V:Si=6:5. (1) 14 V/cm, (2) 17.5 V/cm and (3) 22 V/cm.

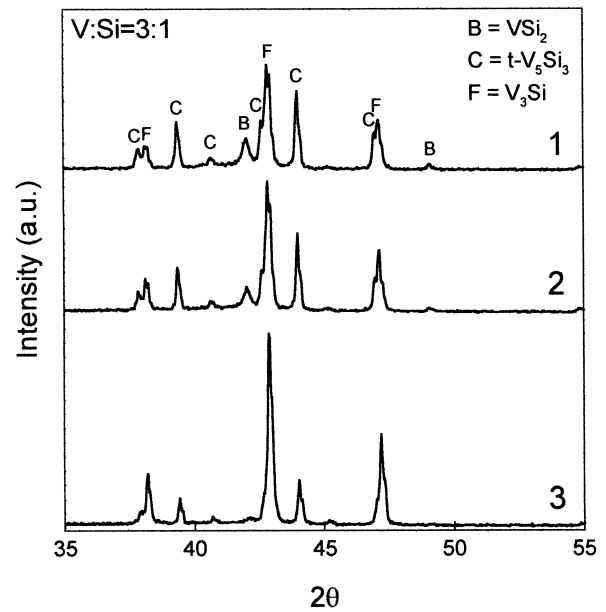


Fig. 9. X-ray powder patterns for the FACS reaction products corresponding to the composition V:Si=3:1. (1) 9 V/cm, (2) 13 V/cm and (3) 18 V/cm.

compositions, including V:Si=5:3 which sustains a wave even in the absence of a field when finer powders are used. The quenched samples were sectioned either longitudinally and analyzed through SEM and EMPA or sectioned perpendicular to the propagation direction and the various sections examined by XRPD.

Fig. 10a shows a low magnification image of the region across the quenched front for a sample of composition V:Si=1:2. Three zones are discernible, as delineated by the dashed white lines. The first zone, which corresponds to the region ahead of the reaction front (Fig. 10b), contains only the reactants: the bright V grains are surrounded by the darker Si particles. As indicated above, the Si particles are relatively small, 1–5 μm , and the vanadium particles are relatively large, up to 50 μm . No indication of any interaction between the two elements can be observed. The second zone, Fig. 10c, corresponds to the leading edge of the combustion front. The passage of the combustion front is indicated by the sudden appearance of product layers around the V grains. Two layers can be distinguished, the most conspicuous is that of VSi_2 . The second is a thin layer of V_5Si_3 which is situated between the VSi_2 layer and the unreacted vanadium core. The morphology of the product layers suggests that an interaction between solid V and liquid Si has occurred. However, Si grains are still clearly discernible indicating that melting of Si has not been massive, but must be localized around the V grains. In zone 3, (Fig. 10d), massive melting of the Si is observed. A single phase VSi_2 product is present not only around the V grains but also in the form of small round precipitates inside the silicon matrix. Interestingly, no V_5Si_3 layer is observed here at the interface

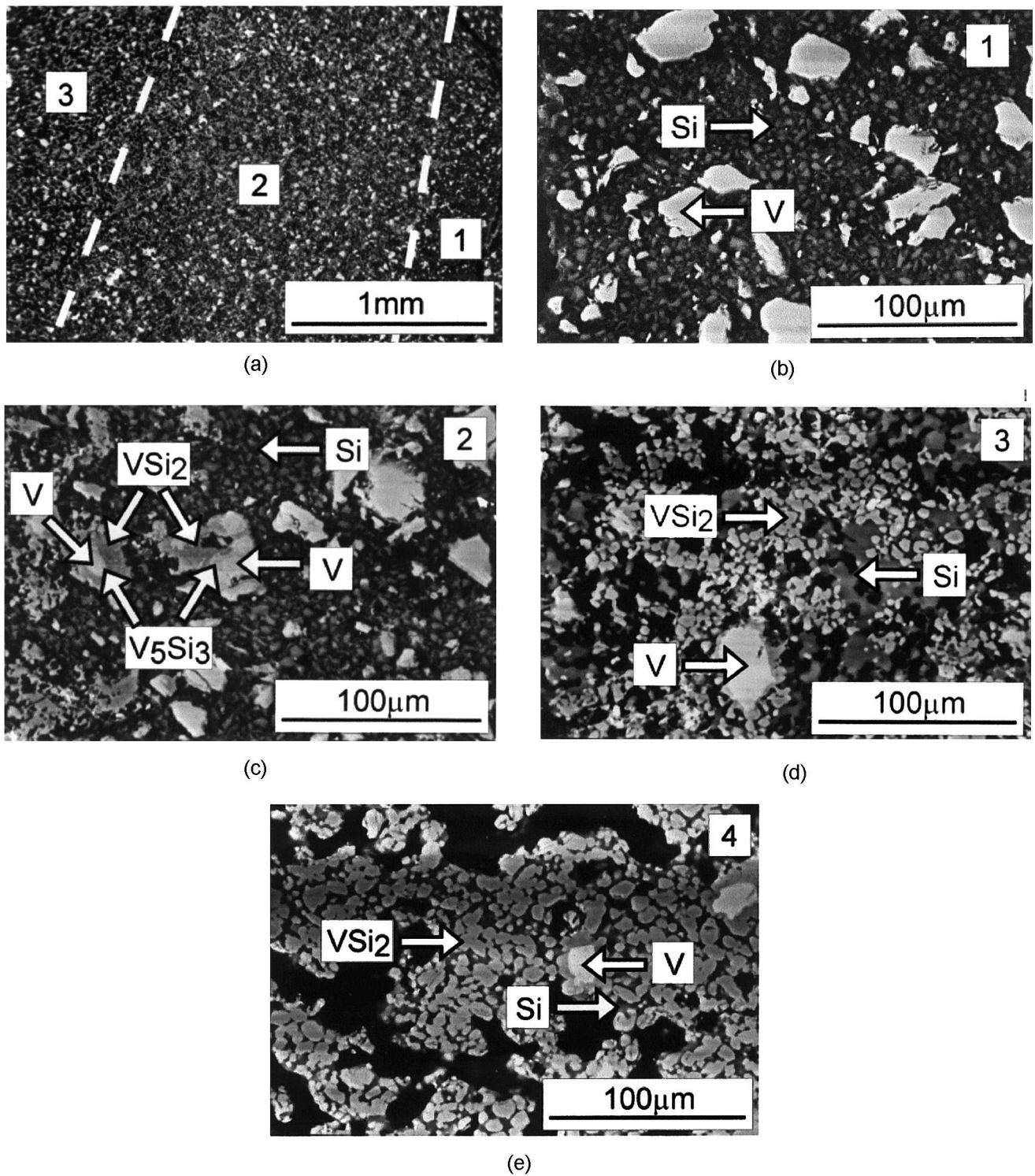


Fig. 10. Microstructure of the FACS quenched product obtained from a V:Si=1:2 starting composition. Zone 1: reactants; Zones 2, 3 and 4: products. SEM backscattered image on metallographic sections.

between VSi_2 and unreacted V. Moving away from the front through the product region (zone 4, not shown in Fig. 10a) only a small amount of residual V can be observed in the matrix of rounded VSi_2 precipitates, Fig. 10e. It should be remembered that in these experiments some residual

(unreacted) V is always observed due to the fact that large particles of vanadium were used as reactant.

Similar sharp quenched fronts have also been observed for the other starting compositions although the microstructural evolution associated with the passage of the

combustion front appears to be somewhat different. As an example we report here the microstructural evolution associated with the reaction of a mixture of composition V:Si=6:5. Fig. 11a shows the low magnification image of the quenched front zone. The region just ahead of the combustion front (zone 1, Fig. 11b) shows the microstructure of the reacting mixture. Also in this case at the leading edge of the quenched reaction front the Si surrounding the V grains melts (zone 2, Fig. 11c) and results in the formation of VSi_2 as first product. In contrast with the case of the composition V:Si=1:2, the main part of the product is observed here around the V grains while only small amounts of VSi_2 precipitates are observed in the melted Si matrix. However, in this case the amount of Si present in the starting mixture is much lower and the V grains appear much more closely spaced. Moving away from the reaction front into the product zone (zone 3, Fig. 11d) we observe the products to form almost exclusively around the residual V grains which are connected to each other by a melted VSi_2 matrix. No silicon is present at this stage and a V_5Si_3 solid product layer starts to grow by a reaction between the melted VSi_2 and the residual V. A much more complex mixture of product phases can be

observed very far from the reaction front, as indicated by the XRPD of the final products (Fig. 8).

As the Si content is reduced in the starting mixture the SEM back-scattered observations become increasingly difficult to evaluate due to the low contrast between the various product phases. For this reason we also made XRPD investigations on sections cut parallel to the quenched reaction front. Three slices 1 mm thick were cut starting from the position corresponding to the leading edge of the combustion front. The first two slices correspond to the zone immediately behind the quenched front, while the third one was obtained from a region well inside the product zone. The slices were then ground and analyzed through XRPD. The results are summarized in Figs. 12–15 for the compositions V:Si of 1:2, 6:5, 5:3 and 3:1, respectively.

The diffraction patterns for the starting composition V:Si=1:2, Fig. 12, agree well with the SEM observations shown in Fig. 10. In all sections, VSi_2 is the only product phase, while the amount of unreacted Si and V diminishes moving away from the front position toward the product zone. The small amount of V_5Si_3 revealed by the SEM observations as a thin layer at the interface between VSi_2

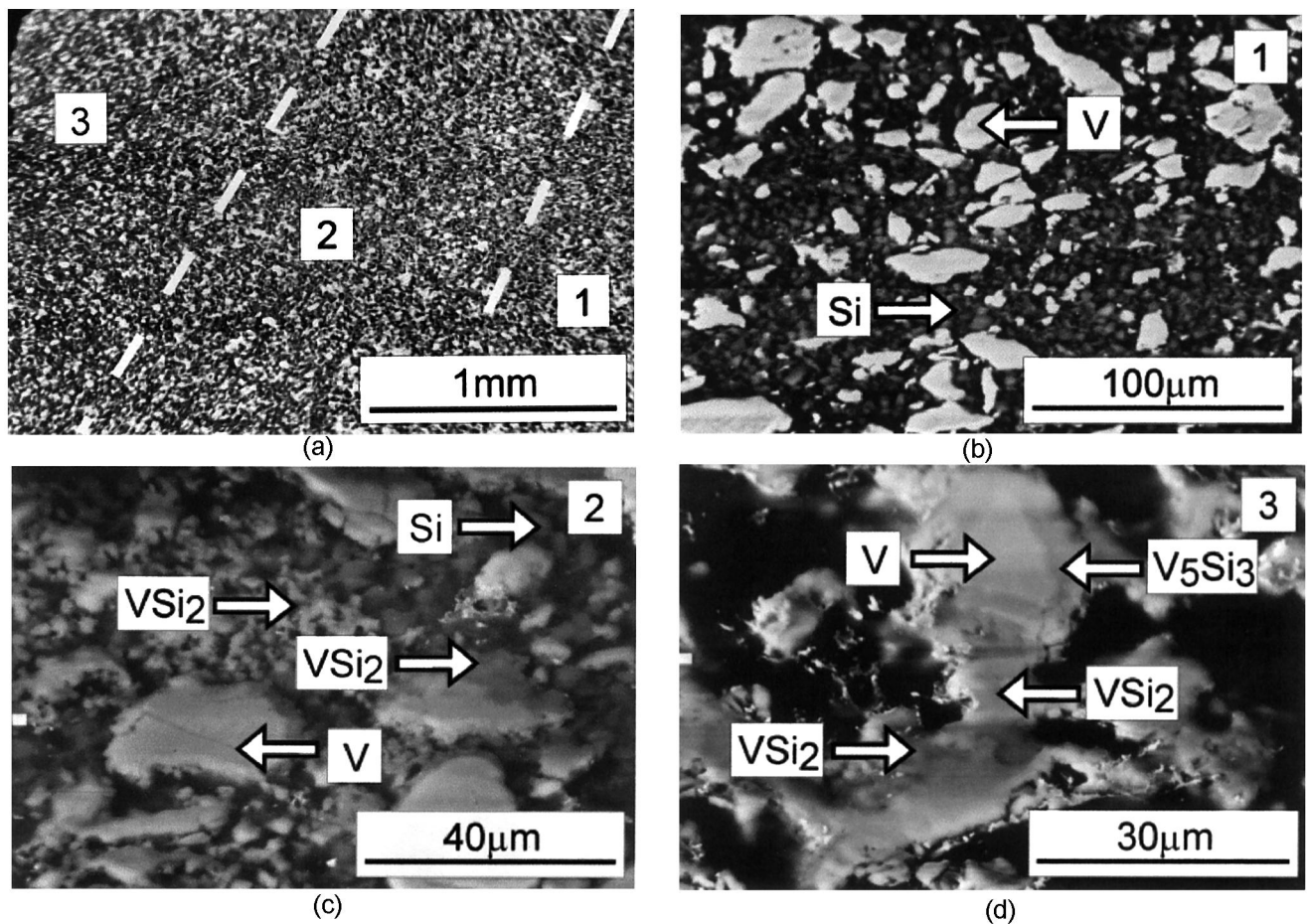


Fig. 11. Microstructure of the FACS quenched product obtained from a V:Si=6:5 starting composition. Zone 1: reactants; Zones 2 and 3: products. SEM backscattered image on polished section.

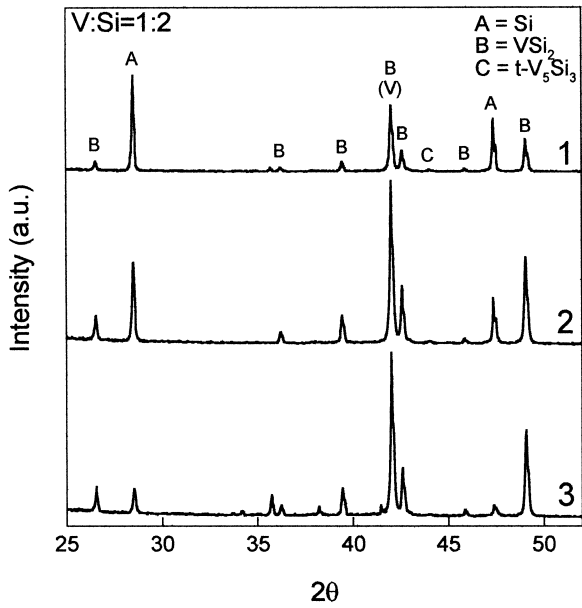


Fig. 12. X-ray powder patterns for the FACS reaction products corresponding to the composition V:Si = 1:2. (1) 0–1 mm behind the quenched front, (2) 1–3 mm behind the quenched front and (3) >3 mm behind the quenched front.

and the unreacted V is not observed here probably because of its relatively small amount. The other compositions (richer in V) confirm that VSi₂ represents the first product of the interaction between Si and V, in agreement with the microscopic observations (see the example of Fig. 11). This phase, in fact, is always the main product in the region corresponding to the leading edge of the combus-

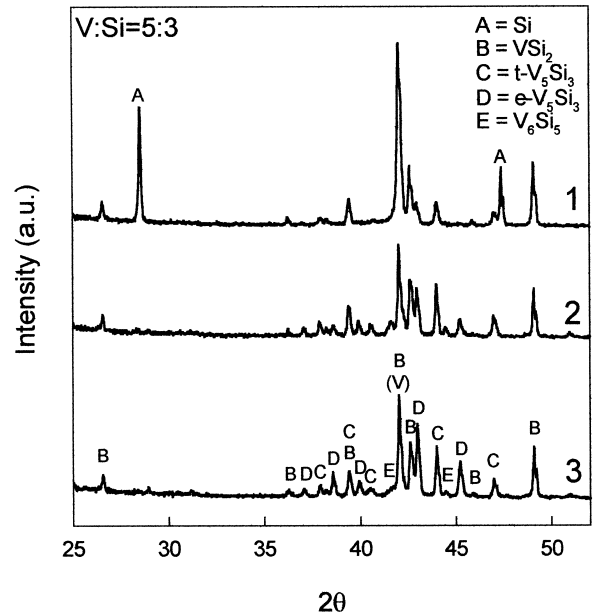


Fig. 14. X-ray powder patterns for the FACS reaction products corresponding to the composition V:Si = 5:3. (1) 0–1 mm behind the quenched front, (2) 1–3 mm behind the quenched front and (3) >3 mm behind the quenched front.

tion front for all V-rich starting compositions (see patterns 1 in Figs. 13–15). Obviously, the relative amount of this phase decreases with an increase in the vanadium content of the starting mixture. In the subsequent layer, corresponding to the region 1–2 mm behind the position of the quenched front, for the mixtures richer in V (Fig. 13), the phase V₅Si₃ in both crystallographic forms starts to grow

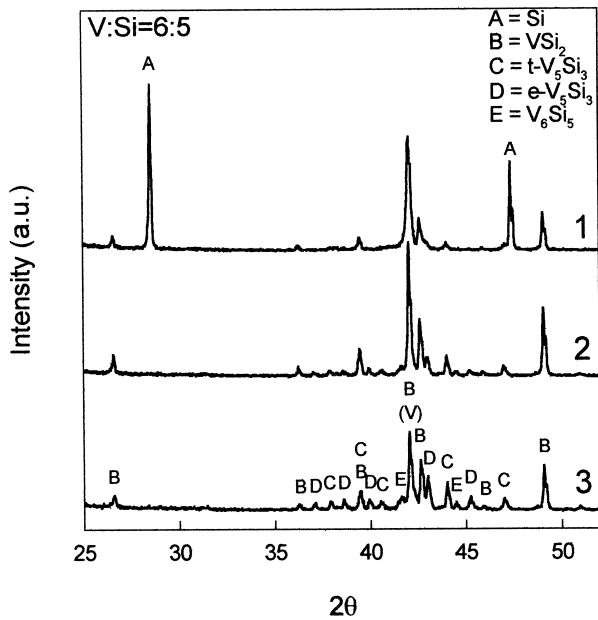


Fig. 13. X-ray powder patterns for the FACS reaction products corresponding to the composition V:Si = 6:5. (1) 0–1 mm behind the quenched front, (2) 1–3 mm behind the quenched front and (3) >3 mm behind the quenched front.

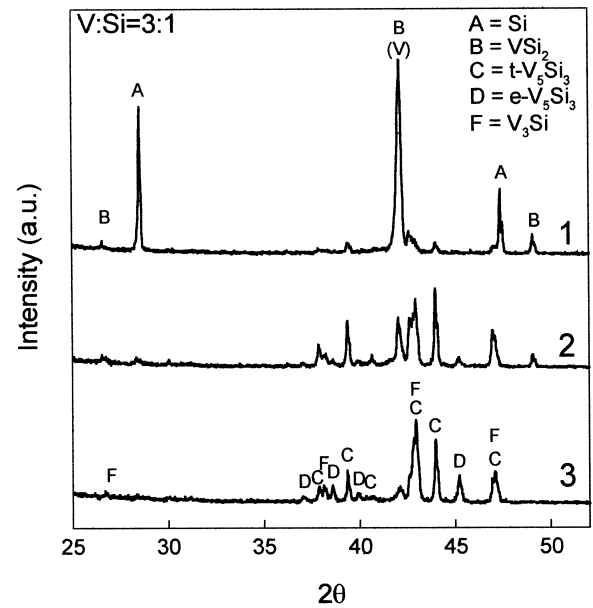


Fig. 15. X-ray powder patterns for the FACS reaction products corresponding to the composition V:Si = 3:1. (1) 0–1 mm behind the quenched front, (2) 1–3 mm behind the quenched front and (3) >3 mm behind the quenched front.

and become the dominant phase. All the other phases begin to appear only in the last section, corresponding to regions several millimeters behind the combustion front.

3.3. Diffusion couples

As indicated above, there is no information in the literature concerning the kinetics of solid–solid and solid–liquid interactions in the V–Si system. For this reason our experimental work included such interactions. We present here only a few qualitative results. A more complete report on the reactivity of this system will be presented elsewhere [16].

Solid–solid isothermal interactions between V and Si were studied by diffusion-couple experiments performed between 1150 and 1350°C. At the lowest temperature (1150°C) a three-layer product was formed (Fig. 16). It includes the phases: VSi_2 at the Si-rich side, V_3Si at the V rich side and V_5Si_3 between them. VSi_2 is by far the most conspicuous phase. The thickness of the VSi_2 and V_5Si_3 layers increase parabolically with time while that of V_3Si did not grow thicker than 1–2 μm [16]. When the temperature was raised to 1250°C and 1350°C a fourth, thin (1–2 μm) layer of V_6Si_5 appeared between the VSi_2 and V_5Si_3 layers, Fig. 17. As for the case of the V_3Si layer, that of V_6Si_5 appears not to grow appreciably with time. It is interesting to observe that the Si-rich layer (VSi_2) appears to be compact and relatively pore-free, while the V-rich layers (V_5Si_3 and V_3Si) contain a significant amount of porosity. Fig. 18 shows the microstructure resulting from the interaction between V and Si when the temperature is raised above the Si melting point. After a 5 min interaction a considerable dissolution of V into liquid Si is observed, as indicated by the large amount of VSi_2 precipitates observed inside the Si matrix. No other phases appear in these precipitates. At the interface between liquid Si and solid vanadium only two layers are observed: a

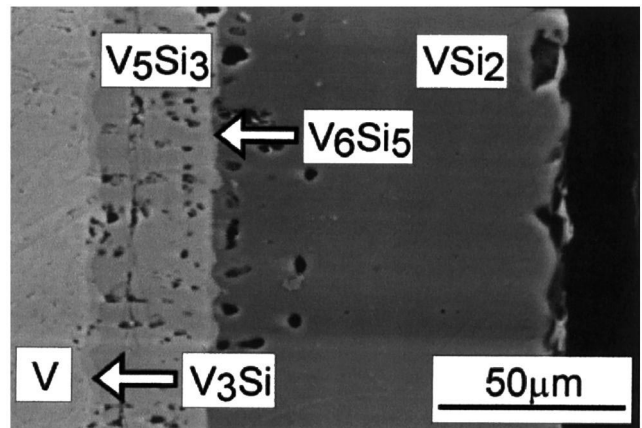


Fig. 17. Backscattered SEM image of a V–Si diffusion couple. $T=1250^\circ\text{C}$, $t=8$ h.

layer of VSi_2 near the Si melt and a thinner layer of V_5Si_3 adjacent to the vanadium.

4. Discussion

It must be first noted that the use of field activation has made it possible to obtain stable combustion fronts for all the compositions corresponding to the intermetallic compounds in the V–Si system. In the absence of a field, stable combustion reactions could only be obtained in the case of the composition V:Si=5:3. In this respect, the applied field showed a strong influence on the macrokinetic characteristics of the combustion processes in this system. On the other hand, the reactions show an unusually weak dependence of the maximum combustion temperature and propagation rates on the intensity of the applied field, with the notable exception of the V:Si=1:2 composition. This is in contrast with the expected increase in Joule heating due to the observed increase in current flow, as has been ex-

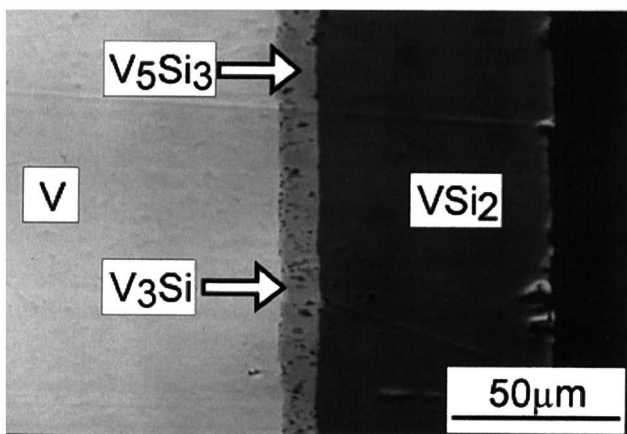


Fig. 16. Backscattered SEM image of a V–Si diffusion couple. $T=1150^\circ\text{C}$, $t=16$ h.

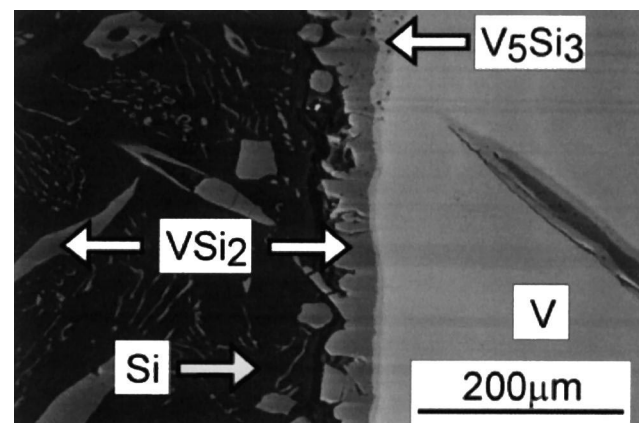


Fig. 18. Microstructure of the product obtained from solid V and liquid Si isothermal reaction. $T=1460^\circ\text{C}$, $t=5$ min. SEM backscattered image on polished section.

perimentally demonstrated in investigations on other silicide systems such as W–Si [9], Nb–Si [12] and Ta–Si [14]. The lack of dependence of the wave velocity and wave temperature on the applied field is likely the consequence of the high electrical conductivity of the product silicide phases. The effect of conductivity on wave temperature and velocity for various field strengths has been simulated for the case of the synthesis of SiC [17]. The results of this modeling study are shown in Fig. 19 for the dependence of the wave velocity on the conductivity factor, F_σ , for SiC (where F_σ is the ratio of the assumed conductivity divided by the real value). The figure shows that for relatively low F_σ values, i.e. for low conducting products, there is a significant increase in the wave velocity with the applied field, in agreement with experimental observation for the case of SiC [18]. However, as the conductivity of the product increases (Fig. 19), the effect of the field becomes less significant. In cases with high conducting products, a major portion of the current is carried in the zone behind the wave and the net effect is that the field contribution to the reaction zone is small. The current–voltage plot of Fig. 5 is typical for a highly conductive product, in which the current continuously increases during the reaction as product volume increases. On the other hand when insulating products are formed, the current density is limited to the front zone and the maximum current value remains practically constant after the initial rise corresponding to the reaction ignition [18]. The temperature profiles shown in Fig. 4 confirm that the current flux occurs only in the product phases. In fact, the increase in field strength produces only an increase in the temperature behind the leading reaction front. The apparently anomalous behavior of the V:Si=1:2 composition can be easily explained considering that in these samples massive melting of the products is always observed; this

produces a large deformation in the reacted part of the sample with a loss of contact with electrodes. As a result the current is forced to flow only in the proximity of the front reacting zone.

Although combustion wave can be initiated in all compositions investigated, only in the cases of V:Si=1:2 and V:Si=5:3 is the product a relatively pure phase with the desired stoichiometry. For the cases of V:Si=3:1 and V:Si=6:5 the product was more complex, containing several phases. Since the differences in ΔH_f values between the four compounds are not very pronounced, the feasibility of their formation cannot be directly related to thermodynamic stability. As for other intermetallic systems [8,13,14] an overriding role of the kinetic parameters on thermodynamic stability must be considered. For this reason solid–solid diffusion couples and solid–liquid experiments were important despite the large differences between these isothermal experiments and the non-isothermal conditions in combustion synthesis. These measurements gave indications of the nucleation and growth characteristics of the possible phases. The phases VSi_2 and V_5Si_3 were by far the fastest growing phases in case of solid–solid interaction and the only ones obtained in solid–liquid experiments. The amount of V_6Si_5 and V_3Si observed in solid-state diffusion couples is extremely limited while these phases are totally absent in solid–liquid experiments, where the reaction time is considerably shorter. These results suggest that the difficulty in obtaining such phases by FACS is mainly kinetic in nature.

These conclusions agree well with the observations obtained from quenched combustion experiments. These experiments, in fact, provide quite a clear picture on the reaction path during the passage of the combustion wave. The first event of the interaction between V and Si appears to be the formation of some liquid phase and the resulting solid–liquid interaction appears to be the process controlling the overall reaction. The details of the interaction seem to depend to some extent on the stoichiometry of the starting mixture. In the case of V:Si=1:2 samples, for instance, VSi_2 represents the only product except for the small amount of V_5Si_3 always observed at the interface between the VSi_2 phase and the unreacted V. Melting of Si seems to be initially limited to the region surrounding the V grains. But after massive melting of Si, the VSi_2 product appears in the form of rounded precipitates in the Si matrix, while only a small portion of the product surrounds the residual vanadium grains. This suggests that no phases other than VSi_2 can form from the interaction between liquid Si and solid V until all Si has been consumed. This conclusion is partially confirmed by the isothermal solid–liquid experiments (see Fig. 18) even though, in this case, a small amount of V_5Si_3 is formed at the V interface. However, it must be noted that solid–liquid experiments were performed at a temperature just above the melting point of Si. At such a temperature the solubility of V in liquid Si is quite small (≈ 10 at.%) and saturation of the Si

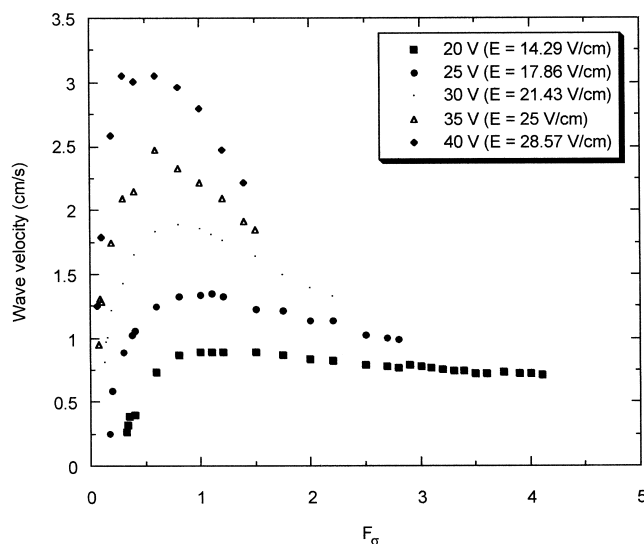


Fig. 19. Modeling results on the effect of electrical conductivity on wave velocity in the synthesis of SiC.

pool is quickly obtained. Saturation effects explain also the presence of some V_5Si_3 on the leading edge of the quenched front in the case of the starting composition V:Si=1:2 (Fig. 10c) and its absence in the later stages of the process (Fig. 10d–e). In the very early stages of the interaction, the melting of Si appears to be limited to a small region around the V grains. These limited liquid regions will be obviously saturated with V and the formation of a phase richer in V (V_5Si_3) is expected. As the massive melting of all the unreacted Si is observed (in the later stages), no saturation can be reached, due to the insufficient amount of available V, and only the VSi_2 phase is observed. These considerations support the previous conclusion that VSi_2 represents the only phase resulting from the interaction between liquid Si and solid V, with all the other phases resulting from subsequent processes which become active only after saturation of the available Si.

In the case of mixtures richer in V, the free silicon is consumed right after the passage of the combustion front. The interaction must continue by a reaction between the VSi_2 (here present in liquid phase) and the residual V to form the other phases. As V-rich phases begin to form, solid state diffusion through such product phases will be the rate-limiting step of the reaction since their melting points are well above the combustion temperatures. This reduces the overall kinetics, and higher temperatures are required in order to take the process to completion. The V:Si=5:3 composition forms a single phase product, but in this case the temperature was considerably higher than for the other compositions. Moreover, V_5Si_3 is the second fastest growing phase, as the diffusion couple experiments indicate. The remaining two compositions (V:Si=6:5 and V:Si=3:1) follow a reaction path similar to that described for V_5Si_3 but in this case the relatively low reaction temperature coupled with the very low intrinsic growth rate of these phases lead to the formation of a highly polyphasic product. The formation of these phases, however, takes place well behind the combustion front, during the sample cooling stage.

The behavior of the V:Si=3:1 composition is in agreement with the preceding consideration. In this case a clear dependence of the product composition on the applied field was observed. Even though the dependence of the front temperature does not seem to be affected by an increase in the applied field, it must be kept in mind that the process is

completed in the post front region, and only a limited amount of product is formed at the combustion front. An increase in the applied field leads to an increase in the current that flows in the products region. As a result, the cooling process is much faster at lower voltages leading to a lower degree of conversion. The fact that a similar dependence of product composition on the applied field was not observed for the V:Si=6:5 composition is probably related to its extremely low growth rate and, in part, to its metastability at room temperature.

Acknowledgements

This work was supported by a grant from Italian Ministry for University and Research (MURST). One of us (ZAM) acknowledge a support from NSF.

References

- [1] A.R. Sarkisyan, S.K. Dolukhanyan, I.P. Borovinskaya, A.G. Merzhanov, *Comb. Explos. Shock Waves* 14 (1978) 49–55.
- [2] A.R. Sarkisyan, S.K. Dolukhanyan, I.P. Borovinskaya, *Poroshk Metall.* 6 (1978) 14–18.
- [3] A.R. Sarkisyan, S.K. Dolukhanyan, I.P. Borovinskaya, *Comb. Explos. Shock Waves* 15 (1979) 95–97.
- [4] S. Zhang, Z.A. Munir, *J. Mater. Sci.* 26 (1991) 3685–3688.
- [5] S. Deevi, *Mater. Sci. Eng.* A149 (1992) 241–251.
- [6] S.B. Bhaduri, R. Radhakrishnan, Z.B. Qian, *Script. Metall. Mater.* 29 (1993) 1089–1094.
- [7] J. Subramanyam, R. Mohan Ran, *Mater. Sci. Eng.* A183 (1994) 205–210.
- [8] N. Bertolino, U. Anselmi-Tamburini, F. Maglia, G. Spinolo, Z.A. Munir, *J. Alloys Comp.* 288 (1999) 238–248.
- [9] S. Gedeveanishvili, Z.A. Munir, *J. Mater. Res.* 10 (1995) 2642–2647.
- [10] S. Gedeveanishvili, Z.A. Munir, *Mater. Sci. Eng.* A211 (1996) 1–9.
- [11] I.J. Shon, Z.A. Munir, K. Yamazaki, K. Shoda, *J. Am. Ceram. Soc.* 79 (1996) 1875–1880.
- [12] A. Feng, Z.A. Munir, *J. Am. Ceram. Soc.* 80 (1997) 1222–1230.
- [13] F. Maglia, U. Anselmi-Tamburini, N. Bertolino, C. Milanese, Z.A. Munir, *J. Mater. Res.* 15 (2000) 1098–1109.
- [14] F. Maglia, U. Anselmi-Tamburini, N. Bertolino, C. Milanese, Z.A. Munir, *J. Mater. Res.* 16 (2001) 535–544.
- [15] J.F. Smith, *Bull. Alloy Phase Diag.* 6 (1985) 266–271.
- [16] N. Bertolino, F. Maglia, C. Milanese, U. Anselmi-Tamburini, unpublished.
- [17] E.M. Heian-Carrillo, O.A. Graeve, A. Feng, I.A. Faghieh, Z.A. Munir, *J. Mater. Res.* 14 (1999) 1949–1958.
- [18] A. Feng, Z.A. Munir, *Metall. Trans.* 26B (1995) 587–593.